A Model Predictive Control System for Different Phases of a Plasma Discharge in DEMO Tokamak

Gaetano Tartaglione* Roberto Ambrosino† Marco Ariola* Wolfgang Biel‡

Luigi E. Di Grazia§ Massimiliano Mattei† Adriano Mele ¶

April 29, 2023

Abstract

This paper deals with the use of a model predictive control technique to perform the magnetic confinement of a plasma in the DEMO tokamak. We show how to adapt the proposed strategy for the different phases, and hence different goals, of the plasma discharge and how to take into account the constraints that characterize the normal operations of a nuclear fusion reactor. We validate the performance of the proposed control system by using a nonlinear evolution code describing the plasma in a tokamak.

1 Introduction

Recent results in the field of experimental nuclear fusion technology have had a strong media impact; improvement in the field, due to the work of the scientific community, have been demonstrated by results from the latest DT campaign at JET [12] (where a 5 s long pulse produced 16.4 kWh of energy, doubling the previous record), the breakthrough experiment of the NIF facility (where the energetic breakeven condition has been observed for the first time) and the Reinforcement Learning based controller tested by Deep Mind and EPFL-SPC [16].

Moreover, different long range plans for producing electric power from nuclear fusion are in progress. According to the road-map developed by the EUROfusion consortium [17], the International Thermonuclear Experimental Reactor (ITER) [24] is currently under construction. After ITER, the next generation European device will be DEMO [18], i.e. the DEMOnstration Fusion Power Plant, which is currently in the design stage, and it will demonstrate the possibility of producing electric power from nuclear fusion by the middle of this century.

Energy from nuclear fusion reactions is obtained from the combination of low-mass nuclei to form more massive nuclei. In order to carry out the fusion reactions, a fully ionized gas called *plasma* is obtained in a fusion reactor by heating hydrogen isotopes up to $\sim 100M$ degrees.

Modern fusion reactor are based on tokamaks, which are pulsed machines; in each pulse the plasma is created, then its current is ramped up to a reference constant value, the *flat-top* current, then the plasma equilibrium is maintained for a time long enough to achieve a positive energy balance, finally the current is ramped down and the plasma is terminated. During the pulse, the confinement of the plasma is performed by exploiting *magnetic confinement techniques* based on the interaction between the charged particles of the plasma and an external magnetic field generated by currents flowing in suitable coils.

Next generation devices, like ITER and DEMO, must be capable of advanced modes of tokamak operation, hence they need a high performance *magnetic control system* to control the plasma current and position to keep and to maintain a self-sustaining fusion reaction for long duration.

This paper describes the design of a magnetic control system for DEMO tokamak based on the use of a Model Predictive Control (MPC) technique [11]. A preliminary version of this MPC-based controller has been presented in [25] and it enabled the control of the plasma current and shape during the flat-top phase. Now by keeping the features of MPC technique, e.g. the controller can take into account voltages and currents constraints on the active coils, we propose a controller that can be adapted to the different phases of the plasma discharge, and it can be integrated with a control system

---

*Dipartimento di Ingegneria, Universitá degli Studi Napoli "Parthenope", 80143 Napoli, Italy.

†DIETI, Università degli Studi di Napoli Federico II, 80125 Napoli, Italy.

‡Institut für Energie und Klimaforschung, Forschungszentrum Jülich GmbH, Germany.

§L. E. di Grazia is with CREATE consortium, 80125 Naples, Italy.

¶DEIM, Università degli Studi della Tuscia, 00110 Viterbo, Italy.

for the currents of the active coils, in order to take into account also the pre-programmed currents of the pulse [6].

In the past, others control systems were proposed for DEMO tokamak, see [7, 9], by implementing linear control techniques and their performance was verified to be satisfactory in case of external disturbances and saturation in the actuators. Here using an MPC based approach, we obtain better performance by taking into account constraints during the design phase of the controller.

The rest of this paper is organized as follows. In Section 2 we present the layout of the tokamak and its linearized model is obtained. In Section 3 the architecture of the overall magnetic control system is detailed, whereas Section 4 is dedicated to the presentation of the vertical stabilization and of the current controllers. In Sections 5 we describe the MPC-based controller. In Section 6 the performance of the proposed controller are evaluated by analyzing results of a simulation based on validated nonlinear evolution code. Finally, in Section 7 some conclusions are drawn.

2 Plasma modelling for magnetic control

As said in Section 1, DEMO is currently in the design stage and different layouts for its vessel were presented in the past. In this work we consider the single null baseline configuration proposed in 2017 [19] and shown in Fig. 1. In this configuration, the poloidal cross-section of the vessel is composed by 11 *ex-vessel* coils and 2 *in-vessel* coils.

The ex-vessel coils are located outside the vessel and they are supposed to be superconductive coils and to be fed by the so-called main converters. According to the layout in Fig. 1, the ex-vessel coils provide six poloidal field coils (named PF1-6) and a central solenoid segmented into five different coils, named CS1, CS2 U/L (upper and lower) and CS3 U/L. The in-vessel coils (named IV1-2) are installed inside the vessel and they are assumed to be copper coils and to be connected in anti-series, so as to produce an approximately radial magnetic field; these coils are fed by a VS dedicated converter.

In this paper we use a model based approach for the design of the control system, hence we need a mathematical model which is able to describe the behavior of the plasma confined in the considered tokamak machine. Magneto Hydro Dynamics (MHD) provides the time evolution of a plasmas confined in a tokamak machine [22]. A common procedure to derive a linear model of the plasma is to linearize the equations of the MHD theory around an equilibrium point [1, 2], which is defined by constant plasma current profile parameters, i.e.
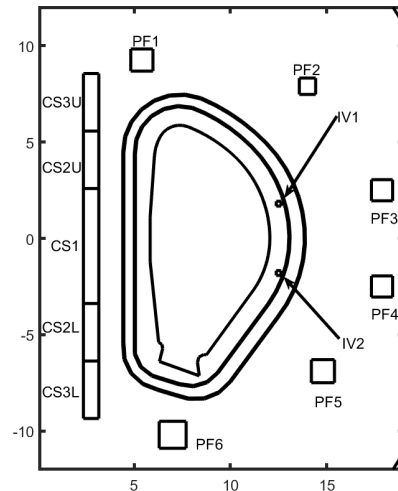

Figure 1: Poloidal cross-section of the DEMO vessel with the active PF coils (black lines).

fixed poloidal beta β_p and internal inductance l_i.

Starting from the layout configuration of the tokamak and by using a linearization tool, interaction between plasma, active coils and passive structures of the machine can be provided in the following linear form, as shown in [6, Section 2.5],

$$(2.1) \qquad L\frac{dI_c(t)}{dt} = -RI_c(t) + V(t) \,,$$

where $I_c(t) \in \mathbb{R}^n$ and $V(t) \in \mathbb{R}^n$ are, respectively, the current and the voltage vectors, L and R are, respectively, the mutual inductance matrix and the resistance matrix, which are estimated by the linearization tool.

The current and voltage vectors can be partitioned as follows

$$I_c(t) = \begin{bmatrix} I_a^T(t) & I_e^T(t) & I_{pl}(t) \end{bmatrix}^T \,,$$
$$V(t) = \begin{bmatrix} V_a^T(t) & 0^T & 0 \end{bmatrix}^T \,,$$

by considering the currents in the active circuits $I_a(t) \in \mathbb{R}^{12}$, the eddy currents $I_e(t) \in \mathbb{R}^{n_e}$, the plasma current $I_{pl}(t) \in \mathbb{R}$ and the input voltages $V_a(t) \in \mathbb{R}^{12}$. Note that only the active coils can be voltage-driven. Moreover, considering the location-based partitioning of the active coils, we can distinguish the quantities of the ex-vessel circuits from those of the in-vessel circuits

$$I_a(t) = \begin{bmatrix} I_{EX}^T(t) & I_{IN}(t) \end{bmatrix}^T \,,$$
$$V_a(t) = \begin{bmatrix} V_{EX}^T(t) & V_{IN}(t) \end{bmatrix}^T \,.$$

Finally, by using the linearization tool we can obtain

a linear output equation

(2.2)
$$y(t) = C_{lin} I_c(t),$$

where the output vector $y(t) \in \mathbb{R}^p$ includes the quantities which are fed-back by the control system, while the output matrix $C_{lin} \in \mathbb{R}^{p \times n}$ is obtained by the linearization tool.

3 Architecture of the magnetic controller

Since DEMO will have to accomplish all advanced modes of a nuclear fusion plant, its magnetic control system must ensure the proper vertical stabilization of the plasma, and simultaneously it must ensure the proper control of the plasma shape and current.

We solve the vertical stabilization problem by considering the stabilizing strategy proposed in [25] and based on the use the in-vessel coils. This approach ensures a faster response than the one based on the use of the ex-vessel coils, since the electromagnetic field generated by the in-vessel coils does not have to penetrate the structures of the tokamak.

A cascade approach is developed to solve the plasma current and shape control problem. This approach is carried out by implementing a dedicated controller for the currents of the ex-vessel active coils. In this way, the references for the ex-vessel coil currents are computed by an outer-loop controller in order to perform the control of the plasma shape and current. In this work, both control loops are developed by exploiting model-based approaches.

The architecture of the proposed magnetic control system is shown in Figure 2, and is characterized by the following subsystems: (i) the vertical stabilization controller, which computes the voltage V_{IN} needed to vertically stabilize the plasma; (ii) the controller for the currents of the ex-vessel coils, which decouples and controls the dynamics of the currents of the PF and CS coils; (iii) the MPC controller, which computes the currents needed to control the plasma current and shape, and to track the feed-forward quantities related to the specifications of the scenario.

4 VS controller and current controller

For the vertical stabilization problem we consider the solution presented in [25], which exploits the in-vessel coils presented in this configuration of the tokamak. In particular, by considering the anti-series connection among the in-vessel coils, the vertical stability controller is defined by a control law that computes the voltage for the in-vessel coil $V_{IN}(t)$ from the measurements of the plasma vertical velocity $\dot{z}_c$ and the in-vessel coil
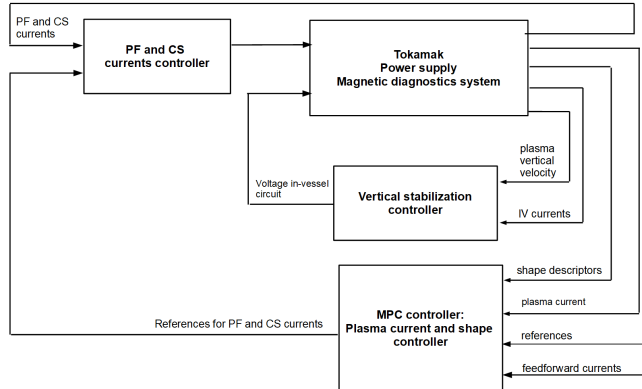

Figure 2: Architecture of the proposed control system based on an MPC controller.

current I_{IN}

(4.3)
$$V_{IN}(t) = K_1 \dot{z}_c(t) + K_2 I_{IN}(t),$$

where control gains K_1 and K_2 are fixed in order to maximize the robustness properties of the closed loop system [15].

The design of the PF and CS currents controller is carried out by considering a model-based approach, starting from the model of the stabilized plasma through the control law (4.3). Indeed, via a singular perturbation decomposition [23], we can obtain a reduced-order model by considering that the eddy currents are characterized by a much faster evolution than the currents flowing in the ex-vessel coils. Hence, the following reduced-order model can be used to approximate the dynamics of the ex-vessel coils currents

(4.4)
$$L_{EX} \dot{I}_{EX} = V_{EX},$$

where $L_{EX} \in \mathbb{R}^{11 \times 11}$ is a submatrix of the mutual inductance matrix.

The model (4.4) has been used to design the current controller and in order to decouple them, the following control law has been considered

(4.5)
$$V_{EX}(t) = L_{EX} \Lambda \left(\tilde{I}_{EX}(t) - I_{EX}(t) \right)$$

where $\tilde{I}_{EX}(t)$ is the vector of the current references and $\Lambda = I_{11}/\tau$, being $\tau > 0$ a design parameter.

5 MPC controller

In this Section we propose the main result of this work: an MPC controller which is able to perform control of the plasma current and shape during different phases of the plasma discharge.

In the past, two strategies were developed for controlling the plasma shape [6]: the former is based on controlling the magnetic flux in a finite number of points in the vessel (*isoflux control approach*), the latter is based on controlling the plasma-wall distance along a finite number of directions (*gap control approach*). Typically these approaches are used in different phases of a plasma discharge. Isoflux control approach is particularly useful to control the shape of a plasma characterized by a limiter configuration and during the transition phases from a limited configuration to a diverted one and vice versa. Gap control approach is particularly useful to control the shape of a plasma characterized by a diverted configuration, hence during the ramp-up, ramp-down and flat-top phases.

The isoflux approach is performed by specifying a set of target boundary points for the shape and the coil currents are adjusted so that the flux at these points is equal to the flux at a reference point. The reference point is chosen as the target X-point in the diverted configuration. Moreover, in order to make the transition happen in the selected region, the components of the magnetic induction field are controlled to zero at the target X-point position.

The gap control approach is adopted by controlling a finite set of geometrical gaps between the plasma boundary and the wall of the vessel. The desired shape is defined by fixing the reference values for the controlled gaps. Hence the coil currents are adjusted so that gaps follows the references values.

The proposed MPC controller allows us to switch between these control approaches based on the real time estimation of the plasma configuration during the discharge. The controller is able to switch to the gap control approach when the plasma accomplishes the transition to the diverted configuration. Both the control approaches require the solution of an output tracking problem, which can be tackled in the MPC context by recasting the prediction model in a *velocity form* [8], as explained in the following section.

5.1 Prediction model The prediction model is obtained from the reduced-order model 4.5

$$(5.6a) \quad L_{EX}\frac{dI_{EX}}{dt}(t) = L_{EX}\Lambda\left(\tilde{I}_{EX}(t) - I_{EX}(t)\right),$$
$$(5.6b) \quad y(t) = C_{EX}I_{EX}(t),$$

the output vector $y(t)$ includes the quantities which are needed to achieve the plasma current and shape control approach, hence it includes the components of the magnetic induction field $B_r(t)$ and $B_z(t)$ at the target X-point, the magnetic flux $\psi(t)$ at target boundary points, the controlled plasma-wall distances $g(t)$ and

the plasma current $I_{pl}(t)$. Matrix C_{EX} is obtained by estimating the effects of the currents in the active coils on the output variables by using the linearization tools, more details can be found in [25].

To obtain a discrete-time prediction model, we perform a standard bilinear transformation to the model (5.6), and by setting a suitable sample time T we obtain

$$(5.7a) \quad x(t_{k+1}) = Ax(t_k) + Bu(t_k),$$
$$(5.7b) \quad y(t_k) = Cx(t_k),$$

where matrices A, B and C are computed from the matrices of the continuous-time model (5.6). The discrete-time system (5.7) is characterized by the state and input vectors containing the currents of the ex-vessel active coils and their reference values, respectively.

Now, in order to achieve an output tracking controller, system (5.7) is recast in the so-called *velocity form* [8] by introducing the variables

$$\delta x(t_k) = x(t_k) - x(t_{k-1}),$$
$$\delta u(t_k) = u(t_k) - u(t_{k-1}),$$
$$e(t_k) = y(t_k) - r,$$

where the vector $r \in \mathbb{R}^p$ holds the reference values for the output variables. Hence, system (5.7) can be rewritten in a matrix form as

$$(5.8) \quad \zeta(t_{k+1}) = \mathcal{A}\zeta(t_k) + \mathcal{B}\delta u(t_k),$$

where

$$\zeta(t_k) = \begin{bmatrix} \delta x(t_k) \\ e(t_k) \end{bmatrix}, \ \mathcal{A} = \begin{bmatrix} A & 0 \\ CA & I \end{bmatrix}, \ \mathcal{B} = \begin{bmatrix} B \\ CB \end{bmatrix}.$$

5.2 Optimization problem The optimization problem that characterizes the proposed model predictive controller will be defined below. In particular, at each discrete time instant, the control signals are obtained from the solution of the following linear-quadratic optimization problem, which defines a convex problem,

$$(5.9a) \quad \min_{U(t_k)} J(U(t_k), \zeta(k), U_{ff}(t_k), N),$$
$$\text{s.t.}$$
$$(5.9b) \quad \zeta(t_{k+1}) = \mathcal{A}\zeta(t_k) + \mathcal{B}\delta u(t_k),$$
$$(5.9c) \quad \Delta_{min} \le U(t_k) \le \Delta_{\max},$$
$$(5.9d) \quad A_c U(t_k) \le b_c(t_k),$$

where

$$U_{ff}(t_k) = \begin{bmatrix} \delta u_{ff}^T(t_k) \ \delta u_{ff}^T(t_{k+1}) \ \cdots \ \delta u_{ff}^T(t_{k+N-1}) \end{bmatrix}^T,$$

is the sequence of variations of the feed-forward currents over the prediction horizon and

$$U(t_k) = \left[\delta u^T(t_k) \ \delta u^T(t_{k+1}) \ \cdots \ \delta u^T(t_{k+N-1}) \right]^T ,$$

is the optimal sequence of variations of control inputs over the prediction horizon.

In (5.9a), $J(U(t_k), \zeta(t_k), U_{ff}(t_k), N)$ is a quadratic performance index defined as

$$(5.10) \quad J(U(t_k), \zeta(t_k), U_{ff}(t_k), N) =$$
$$\sum_{i=1}^{N-1} \zeta^T(t_{k+i}) Q(t_k) \zeta(t_{k+i}) + \sum_{i=0}^{N-1} \left(\delta u(t_{k+i}) - \right.$$
$$\left. \delta u_{ff}(t_{k+i}) \right)^T R(t_k) \left(\delta u(t_{k+i}) - \delta u_{ff}(t_{k+i}) \right) +$$
$$\zeta^T(t_{k+N}) S(t_k) \zeta(t_{k+N}) ,$$

where the weighting matrices $Q(t_k), S(t_k) > 0$ and $R(t_k) \geq 0$ are tuning parameters. By minimizing performance index (5.10), we obtain the control sequence that allows us to track the references values of output variables and the feed-forward currents. In particular, tuning matrices $Q(t_k)$ and $R(t_k)$ allow us to affect the performance of the closed-loop system. The matrix $S(t_k)$ defines the terminal cost and its choice influences the closed loop stability.

In the following, we assume at each time instant t_k, the terminal cost matrix $S(t_k)$ is computed as the solution of the following discrete time algebraic Riccati equation

$$(5.11) \quad S(t_k) = Q(t_k) + \mathcal{A}^T S(t_k) \mathcal{A}$$
$$- \left(\mathcal{B}^T S(t_k) \mathcal{A} \right)^T \left(R(t_k) + \mathcal{B}^T S(t_k) \mathcal{B} \right)^{-1} \left(\mathcal{B}^T S(t_k) \mathcal{A} \right) .$$

5.3 Linear constraints Now, from the specifications of the considered application, we obtain the constraints that characterize the optimization problem (5.9).

Constraint (5.9c) allows us to take into account a maximum rate of change of the voltage input related to the performance of the ex-vessel coils converter. In particular, the values Δ_{min} and $\Delta_{\max}$ can be obtained from the dynamic model of the power supplies.

The inequality constraints (5.9d) allow to bring into account the voltages saturation and the limits on the currents variations in the active coils. In the following we will show that matrices A_c and $b_c(t_k)$ can be assembled at each time instant starting from the available measures and the limits of the constrained quantities.

Let $I_{\max} \in \mathbb{R}^{11}$ the vector containing the upper bounds of the currents, from the definition of the vector

$\delta u(t_k)$, it follows that references for the currents coils verify the upper limit over all the prediction horizon

$$\tilde{I}_{EX}(t_{k+i}) \leq I_{\max} \quad \text{for } i = 0, \ldots, N-1 ,$$

if

$$\sum_{j=0}^{i} \delta u(t_{k+j}) \leq I_{\max} - \tilde{I}(t_{k-1}) \quad \text{for } i = 0, \ldots, N-1 .$$

Hence, the control sequence verifies the constraint about the currents upper bounds if

$$A_{c_1} U(t_k) \leq b_{c_1}(t_k) ,$$

where

$$A_{c_1} = \begin{bmatrix} I_{11} & 0_{11 \times 11} & \cdots & 0_{11 \times 11} \\ I_{11} & I_{11} & \cdots & 0_{11 \times 11} \\ \vdots & \vdots & \ddots & \vdots \\ I_{11} & I_{11} & \cdots & I_{11} \end{bmatrix}, b_{c_1} = \begin{bmatrix} I_{\max} - \tilde{I}(t_{k-1}) \\ I_{\max} - \tilde{I}(t_{k-1}) \\ \vdots \\ I_{\max} - \tilde{I}(t_{k-1}) \end{bmatrix} .$$

The lower bounds can be brought into account by computing matrices A_{c_2} and $b_{c_2}(k)$ with a similar approach.

By considering the control law (4.5) of the current controller, we can take into account the voltages saturation. As an example, consider the vector $V_{\max} \in \mathbb{R}^{11}$ containing the voltages upper bounds. From the definition of the vector $\delta u(t_k)$, it follows that voltages needed to track the currents references verify the upper limit

$$V(t_k) = L\Lambda \left(\tilde{I}(t_k) - I(t_k) \right) \leq V_{\max}$$

if

$$L\Lambda \left(\delta u(t_k) + \tilde{I}(t_{k-1}) - I(t_k) \right) \leq V_{\max} .$$

Hence, the control sequence verifies the constraint on the voltages upper bounds if

$$A_{c_3} U(t_k) \leq b_{c_3}(t_k) ,$$

where

$$A_{c_3} = L\Lambda M_c ,$$
$$b_{c_3}(t_k) = V_{\max} + L\Lambda I(t_k) - L\Lambda \tilde{I}(t_{k-1}) ,$$

the matrix M_c allows us to select vector $\delta u(t_k)$ from the control sequence $U(t_k)$. The lower bounds can be brought into account by computing matrices A_{c_4} and $b_{c_4}(t_k)$ with a similar approach.

Hence, matrices in (5.9d) are evaluated as follows

$$A_c = \begin{bmatrix} A_{c_1}^T & A_{c_2}^T & A_{c_3}^T & A_{c_4}^T \end{bmatrix}^T ,$$
$$b_c(k) = \begin{bmatrix} b_{c_1}^T(t_k) & b_{c_2}^T(t_k) & b_{c_3}^T(t_k) & b_{c_4}^T(t_k) \end{bmatrix}^T .$$

We remark that, at each discrete time, the optimization problem (5.9) can be defined over the prediction horizon from the feedback of the measurements of the active coil currents and the tracking errors.

6 Nonlinear simulations

The performance of the proposed magnetic control system have been evaluated by means of nonlinear simulations.

The nonlinear evolution of the plasma confined in the vessel of DEMO have been simulated by using the evolution code CREATE-NL [1]. This code is based on a finite elements method and it simulates the plasma behavior by taking into account the currents of the active coils and the eddy currents in the structures of the vessel. Experimental data from JET plasma [14] were used to validate the code and currently CREATE-NL is used for analysis on existing and future tokamaks such as JET [3], TCV [4], ITER [5], JT-60SA [13] and EAST [10].

To test the performance of the proposed controller, we simulated the initial part of the ramp-up phase of the plasma discharge in DEMO. During this phase of the discharge, the magnetic control system must perform the plasma transition from the limited configuration to the diverted one, while the plasma current is ramped up. The performed simulation starts from the equilibrium configuration at plasma current $I_{pl} = 3.5$ MA, poloidal beta $\beta_p = 0.134$ and internal inductance $l_i = 1.000$. The preprogrammed scenario is obtained by fixing a constant rate of change for the plasma current of $0.1\,MA/s$ and by considering, further the initial equilibrium configuration of the plasma at the current $I_{pl} = 3.5$ MA, also the equilibrium configurations at the currents $I_{pl} = 4.5$ MA and $I_{pl} = 5.5$ MA, both additional configurations are obtained by considering poloidal beta $\beta_p = 0.134$ and internal inductance $l_i = 1.000$. Hence, the feedforward currents and the references for the controlled gaps are obtained from linear interpolations of the equilibrium values among the different configurations. The linear models at different values of plasma model has been computed by using the linear CREATE-L evolution code [2].

Figure 3 shows the quantities that are controlled during the discharge to achieve the plasma shape control. In particular, we have set the target X-point position and the 3 control points for the magnetic flux to perform the isoflux approach, and we have set 5 gaps to perform the gap control approach. We remark that the target X-point and the flux control points have been set by considering the plasma shape at the equilibrium configuration for $I_{pl} = 4.5$ MA. The controlled gaps have been set by considering that the three gaps G1, G2 and G3 allow us to control the distance from the walls of vessel, finally gaps G4 and G5 allow us to control the positions of the strike points.

The simulation have been carried out integrating in the CREATE-NL code a Matlab implementation of the
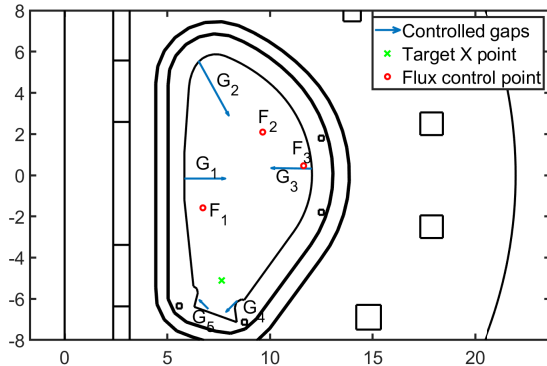

Figure 3: Poloidal cross-section of the DEMO vessel (black lines) with the 5 controlled plasma-wall distances (blue arrows), the 3 flux control points (red circles) and the target X-point (green cross).

presented MPC controller. In particular, for the implementation of the controller we set a sampling time $T = 0.01$ s and a prediction horizon of length $N = 20$. Moreover the optimization problem (5.9) is solved by using the quadratic programming solver $qpOASES$ [21], which is based on an implementation of the Online Active Set Strategy [20], to compute at each discrete time instant the solution of the optimization problem (5.9).

The quadratic performance index (5.10) has been characterized by setting $R = 10^3 \operatorname{diag}(1_{1\times 11})$ and $Q(t_k) = \operatorname{diag}\left(\begin{bmatrix} q_1 & q_2(t_k) & q_3(t_k) & q_4 \end{bmatrix}\right)$, where $q_1 = 1_{1\times 11}$,

$$q_2(t_k) = (1 - \alpha(t_k)) \cdot 10^2 \cdot \begin{bmatrix} 1 & 1 & 12 & 12 & 12 \end{bmatrix},$$
$$q_3(t_k) = \alpha(t_k) \cdot 10^3 \cdot \begin{bmatrix} 20 & 20 & 20 & 2 & 2 \end{bmatrix},$$

and $q_4 = 10^{-4}$. As said, the terminal cost matrix $S(t_k)$ has been computed as solution of the equation (5.11) for the prediction model and the above weighting matrices. The above weights have been set by considering the magnitude of the elements of the state vector $\zeta(t_k)$, and by considering performance specification in tracking constant reference values.

Since vectors q_2 and q_3 weight the tracking errors related to the isoflux control strategy and to the gap control strategy, respectively, we introduced the time-varying parameter $\alpha(t_k)$ in order to switch between the two control strategies when the transition happens. The value of the parameter $\alpha(t_k)$ is based on the estimation of the plasma configuration, that is supposed to be real-time performed, i.e. $\alpha(t_k)$ is equal to 0.999 as long as the plasma is characterized by a limiter configuration, hence $\alpha(t_k)$ linearly varies to 0.001 in 2 seconds starting from the time instant of the X-point making to obtain

a smooth transition, after that the value 0.001 is kept constant.

Different linear prediction models have been used during the simulation by changing the matrices in (5.8) on the base of the plasma configuration. Linear plasma models have been obtained at the equilibrium conditions which have been used to define the preprogrammed scenario. Indeed, before the time instant of the X-point making, we use the linear model at plasma current $I_{pl} = 3.5$ MA, after that we switch to the linear model at plasma current $I_{pl} = 4.5$ MA.

Table 1: Voltages saturation for the CS-PF coils

Coils	Voltage Saturation $[kV]$
CS1	12
CS2 U/L	6
CS3 U/L	6
PF 1-6	9

Matrices of constraint (5.9d) have been defined by considering the voltages and the currents saturation in Table 1.

Figure. 4 shows the evolution of the plasma shape during the simulation. Starting from the limiter configuration in Figure 4a, the isoflux strategy allowed the plasma to perform the transition at the diverted configuration at the time instant 6.6 s, Figure 4b points out that the X-point is made close to the target location. Finally, Figure 4a proves that the gap approach allowed the diverted plasma to track the reference shape. The performance of the shape controller are also demonstrated by the results in Figure 5b, which shows that each gap tracks its own reference signal and they approach the final values.

7 Conclusions

In this paper we have presented a magnetic control system for DEMO based on an MPC technique. The proposed approach can be used during the different phases of the plasma discharge and it allows to brings into account various constraints on the state and input variables. The performed simulation proves the effectiveness of the controller, also with respect to other approaches, previously presented in the literature.

References

[1] R Albanese, R Ambrosino, and M Mattei. CREATE-NL+: A robust control-oriented free boundary dynamic plasma equilibrium solver. *Fusion Engineering and Design*, 96:664–667, 2015.

[2] R Albanese and F Villone. The linearized CREATE-L plasma response model for the control of current, position and shape in tokamaks. *Nuclear Fusion*, 38(5):723, 1998.

[3] G Ambrosino, M Ariola, A Pironti, and F Sartori. Design and implementation of an output regulation controller for the JET tokamak. *IEEE Transactions on Control Systems Technology*, 16(6):1101–1111, 2008.

[4] R Ambrosino, R Albanese, S Coda, M Mattei, J M Moret, and H Reimerdes. Optimization of experimental snowflake configurations on TCV. *Nuclear Fusion*, 54(12):123008, 2014.

[5] R Ambrosino, M Ariola, G De Tommasi, M Mattei, A Pironti, and M Cavinato. Design and nonlinear validation of the iter magnetic control system. In *2015 IEEE Conference on Control Applications (CCA)*, pages 1290–1295. IEEE, 2015.

[6] M Ariola and A Pironti. *Magnetic control of tokamak plasmas*, volume 187. Springer, 2008.

[7] M Ariola, A Pironti, R Ambrosino, M Mattei, W Biel, and T Franke. Simulation of magnetic control of the plasma shape on the DEMO tokamak. *Fusion Engineering and Design*, 146:728–731, 2019.

[8] G Betti, M Farina, and R Scattolini. A robust MPC algorithm for offset-free tracking of constant reference signals. *IEEE Transactions on Automatic Control*, 58(9):2394–2400, 2013.

[9] W Biel et al. Development of a concept and basis for the demo diagnostic and control system. *Fusion Engineering and Design*, 179:113122, 2022.

[10] A Castaldo et al. Simulation suite for plasma magnetic control at EAST tokamak. *Fusion Engineering and Design*, 133:19–31, 2018.

[11] D W Clarke and R Scattolini. Constrained receding-horizon predictive control. In *IEE Proceedings D (Control Theory and Applications)*, volume 138, pages 347–354. IET, 1991.

[12] D Clery. European fusion reactor sets record for sustained energy. *Science (New York, NY)*, 375(6581):600–600, 2022.

[13] N Cruz et al. Control-oriented tools for the design and validation of the JT-60SA magnetic control system. *Control Engineering Practice*, 63:81–90, 2017.

[14] G De Tommasi et al. XSC tools: a software suite for tokamak plasma shape control design and validation.
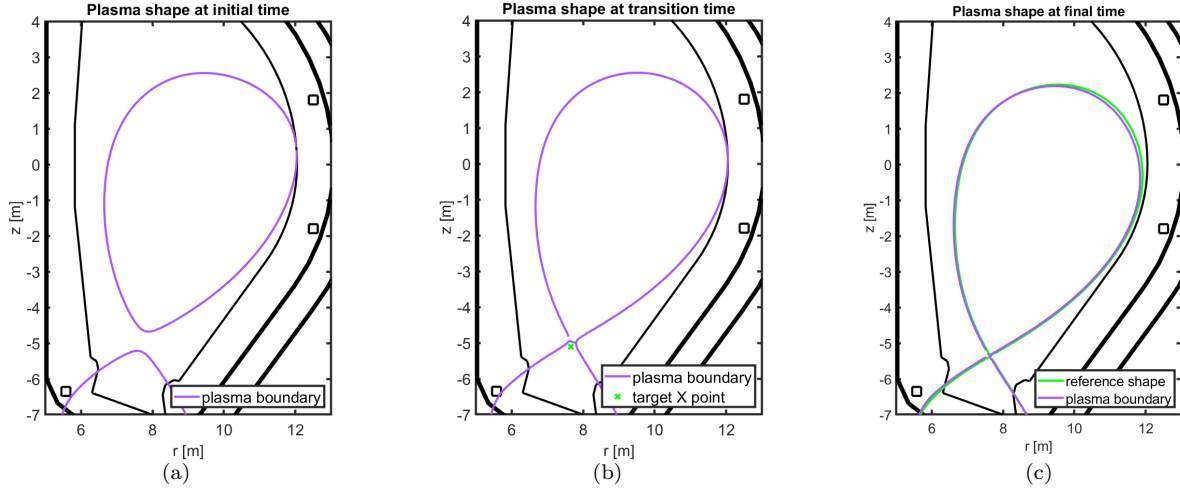
Figure 4: Snapshot of plasma evolution at different time instant: (a) initial time (limiter plasma), (b) formation of the X-point, (c) final time (diverted plasma).
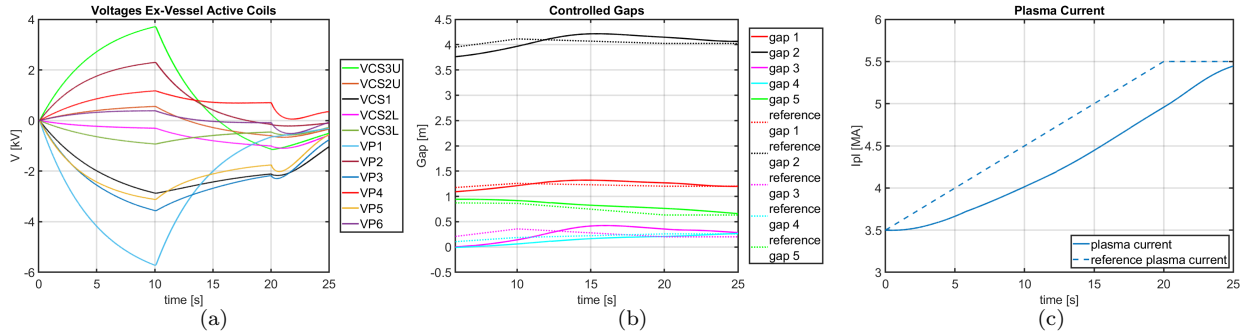

Figure 5: Results of the closed-loop simulation: the voltages on the ex-vessel coils (on the left); the controlled gaps (in the middle); the evolution of the plasma current (on the right).

IEEE transactions on plasma science, 35(3):709–723, 2007.

[15] G De Tommasi, A Mele, and A Pironti. Robust plasma vertical stabilization in tokamak devices via multi-objective optimization. In *International Conference on Optimization and Decision Science*, pages 305–314. Springer, 2017.

[16] Jo Degrave et al. Magnetic control of tokamak plasmas through deep reinforcement learning. *Nature*, 602(7897):414–419, 2022.

[17] T Donnè and W Morris. European Research Roadmap to the Realisation of Fusion Energy. EUROfusion Programme Management Unit, 2018.

[18] G Federici et al. Overview of EU DEMO design and R&D activities. *Fusion Engineering and Design*, 89(7-8):882–889, 2014.

[19] G Federici et al. DEMO design activity in europe: Progress and updates. *Fusion Engineering and Design*, 136:729–741, 2018.

[20] H J Ferreau, H G Bock, and M Diehl. An online active set strategy to overcome the limitations of explicit mpc.

International Journal of Robust and Nonlinear Control, 18(8):816–830, 2008.

[21] H J Ferreau, C Kirches, A Potschka, H G Bock, and M Diehl. qpOASES: A parametric active-set algorithm for quadratic programming. *Mathematical Programming Computation*, 6(4):327–363, 2014.

[22] J P Freidberg. Ideal magnetohydrodynamic theory of magnetic fusion systems. *Reviews of Modern Physics*, 54(3):801, 1982.

[23] P V Kokotovic, J O'Reilly, and H K Khalil. *Singular perturbation methods in control: analysis and design.* Academic Press, Inc., 1986.

[24] J B Lister, A Portone, and Y Gribov. Plasma control in iter. *IEEE Control Systems Magazine*, 26(2):79–91, 2006.

[25] G Tartaglione, M Ariola, W Biel, L E Di Grazia, M Mattei, and A Mele. Plasma magnetic control for DEMO tokamak using MPC. In *2022 IEEE Conference on Control Technology and Applications*, pages 825–830. IEEE, 2022.